EXPLORING SELF-AFFINE MULTIPLICITY VARIABILITY FOR THE EVENTS PRODUCED IN ^{84}Kr + EMULSION COLLISIONS AT RELATIVISTIC ENERGY

M. Sharma, M.K. Singh †

Department of Physics, Institute of Applied Sciences and Humanities
GLA University, Mathura — 281406, India

Received 24 September 2025, accepted 27 January 2026, published online 30 January 2026

The regional variations in multiplicity at relativistic energy multiparticle generation are proposed to be self-affine rather than self-similar due to the anisotropy of phase space. The article uses the two-dimensional factorial moment approach and the Hurst exponent (H) to study self-affine multiplicity fluctuation. At $H = 0.7$, the compound particles and at $H = 0.6$, the shower particles produced in the ^{84}Kr–AgBr collisions and ^{84}Kr–emulsion (^{84}Kr–Em) interact at 1 A GeV and display the best power-law features. All of these data exhibit self-affine multiplicity fluctuation patterns.

DOI:10.5506/APhysPolB.57.1-A4

1. Introduction

In the last decade, researchers have focused a lot of effort on studying relativistic nucleus–nucleus and hadrons–nucleus collisions after the Quark–Gluon Plasma (QGP) was predicted as a new phase of matter [1–6]. The deep properties of nuclear matter, including quarks, gluons, and nuclear matter density, are revealed by heavy-ion collisions, which are used to study a cardinal equation in nuclear and sub-nuclear physics [7–9]. Many investigations on the characteristics of secondary charged particles produced in high-energy nucleus–nucleus collisions have been conducted in recent years [10–14].

Intermittent activity in high-energy nuclear interactions has attracted a lot of attention over the past few decades [15–17]. Once the statistical component has been eradicated, the non-statistical fluctuations may be extracted. It is the phenomena of power-law behavior of scaled factorial

† Corresponding author: singhmanoj59@gmail.com

moments (SFMs) with reducing bin size. Bialas and Peschanski's [18, 19] approach of scaled factorial moments is used to extract the dynamical impact on variations in multiplicity distributions in high-energy reactions in order to comprehend the genesis of non-statistical variations.

The cascade evaporation model, which assumes that statistical stability is reached in the degrading system and that its duration is significantly bigger than the required time to disperse its excited energy among various nucleons in the nucleus, provides a good explanation for the formation of target fragments [17, 20]. According to this model, the hot residual nucleus remains in an excited state shortly after the collision, when the particles that correspond to gray and shower tracks are released from the nucleus. For a thorough grasp of the force and mechanics associated during and soon following nuclear impact, it is crucial to analyze shower particles and target fragments. Mandelbrot suggests that a pattern is referred to as a self-affine fractal whenever it is scaled differently across various directions [17, 21]. To investigate the reaction mechanisms in relativistic energy nuclear collisions, we set up an entirely new particle termed compound particles by combining gray track particles with shower particles.

This study explores the dynamical variations of compound and shower particles released during the interaction between ^{84}Kr–AgBr and ^{84}Kr–Em at 1 A GeV using a two-dimensional SFM technique accounting for phase-space anisotropy. An investigation is conducted into the relationship between the anomalous fractal dimension d_q and the order of instant q.

The SFMs approach is used to analyze the emanating particles intermittent behavior. The scaling behavior of SFMs is influenced by the variability of particle spectra. By introducing a cumulative variable, Bialas and Gazdzicki [22] significantly decreased the distortion of intermittency caused by the non-uniformity of the single particle density ($\rho(x)$) distribution. After that, $\rho(x)$ is connected to the cumulative variable $X(x)$ by

$$X(x) = \int_{x_1}^{x} \rho\left(x'\right) \mathrm{d}x' \Bigg/ \int_{x_1}^{x_2} \rho\left(x'\right) \mathrm{d}x' \,, \tag{1}$$

with x_1 and x_2 being the extremes of distribution $\rho(x)$. $X(x)$ fluctuates between 0 and 1, but $\rho(X(x))$ remains nearly constant. In $\cos\theta$-space, x_1 and $x_2 = -1$ and 1, respectively, while in ϕ-space, they are 0 and 2π, respectively, [17, 23].

An investigation of self-affine multiplicity variation is conducted in a two-dimensional phase space. Assign x_1 and x_2 to the two phase-space parameters and the SFM of the order q will be specified as [17, 23]

$$F_q\left(\delta_{x_1}, \delta_{x_2}\right) = \frac{1}{M}\sum_{m=1}^{M} \frac{\langle n_m(n_m-1)\ldots(n_m-q+1)\rangle}{\langle n_m\rangle^q}\,. \tag{2}$$

A two-dimensional cell has the following dimensions: $\delta_{x_1}, \delta_{x_2}$; the multiplicity and mean multiplicity of the m^{th} cell are n_m and $\langle n_m\rangle$, respectively; and the two-dimensional cells number M with which the one that defines the phase space has been constrained [17, 23].

A two-dimensional area Δ_{x1}, Δ_{x2} is considered, and it is divided into subcells with widths in order to fix δ_{x_1}, δ_{x_2}, and M

$$\delta_{x_1} = \Delta_{x_1}/M_1\,, \tag{3}$$

and

$$\delta_{x_2} = \Delta_{x_2}/M_2\,, \tag{4}$$

$M_1 \neq M_2$ and $M = M_1 \times M_2$ in the x_1 and x_2 directions.

The scale factors that fulfill the equation in this case are M_1 and M_2 [17, 23]

$$M_1 = M_2^H\,. \tag{5}$$

The Hurst exponent, $H = \ln M_1/\ln M_2$ $(0 < H > 1)$, characterizes the diminishing ratios along the x_1 and x_2 directions [23, 24]. Equation (5) reveals that the scale factors M_2 and M_1 cannot exist as integers simultaneously. Therefore, it is appropriate to recognize the elementary space of cell size as a continuously fluctuating number. With a cell size $\to 0$, the self-affine multiplicity variation would reveal as a power-law scaling of $\langle F_q\rangle$

$$\langle F_q\rangle \propto M^{a_q} \tag{6}$$

or a line-based relationship

$$\ln\langle F_q\rangle = a_q \ln M + b\,. \tag{7}$$

An indicator of the severity of the variations in the intermittency exponent is the invariable quantity of the scaling $a_q > 0$ [17, 23].

For the q^{th} order $(q = 2, 3, 4)$, we have computed SFMs with a variable Hurst exponent value in order to investigate the anisotropy structure of phase space [17, 23]. The splitting numbers are selected as follows: $M\phi = 3, 4, \ldots, 30$, and $M\cos\theta$ supplied by and ϕ directions across $\cos\theta$

$$M_{\cos\theta} = M_\phi^H\,. \tag{8}$$

Due to the preserving momentum, which tends to disperse the particles in opposing directions and lower the factorial moment values, we have not taken into account the first two data points, which represent $M\phi = 1, 2$ [23, 25].

2. Experimental details

The nuclear emulsion detector (NED) utilized in this investigation was developed at the GSI in Darmstadt, Germany. Here, NED plates served as both the target and the detector. Very small amounts of I and S are mixed with Ag, Br, O, N, C, and H in NED. NED was created using a ^{84}Kr projectile with 1 A GeV [26]. To find physics events, we used the Olympus BH-2 binocular microscope to scan the NED plate. Two scanning methods are used in the current study: line scanning and volume scanning. The criteria that we utilized to categorize the data after the event collection were range (L), normalized grain density (g^*), and relative velocity (β) [27]. The shower particles with $g^* < 1.4$ and $\beta > 0.7$ are identified as N_s, and they originate from the two interacting nuclei involvement region [28]. Gray particles, denoted by N_g, are emerging from the target spectator region with $0.7 < \beta > 0.3$, $L > 3$ mm, and $6.0 > g^* > 1.4$ [28]. The black particles, indicated by N_b, are emerging from the target spectator region with $\beta < 0.3$, $L < 3$ mm, and $g^* > 6.0$ [28]. The sum of the black and gray particles is referred to as the strongly ionized charged particle (N_h). The AgBr, CNO, and H targets are the three groups into which the emulsion target is separated based on the N_h values. *(i)* The H target has either 0 or 1 N_h values. *(ii)* The range of N_h values for the CNO-target is from 2 to 7. In the case of AgBr target, N_h values exceed 7 [26–28].

3. Result and discussion

The combined variables $X\cos\theta$ and $X\phi$ are utilized in place of $\cos\theta$ and ϕ in order to minimize the impact of the non-flat average distribution [17, 23, 29]. We separated the area [0,1] into $M\cos\theta$–$M\phi$ bins in the $X\cos\theta$–$X\phi$ space. Calculations are performed individually in each of the $M = M\cos\theta \times M\phi$ bins that make up the $\cos\theta$–ϕ space [17, 23]. For the charged-particle multiplicity distribution data set, factorial moments of various orders with diverse values of the Hurst exponent ranging from 0.3 to 1 in steps of 0.1 are computed in order to examine the anisotropic character of the $X\cos\theta$–$X\phi$ phase space [17, 23].

Figure 1 displays the $\ln\langle F_q\rangle$ dependences on $\ln M$ for various orders of the moment at $H = 0.7$ for compound particles emerged from the ^{84}Kr–AgBr (1.7 A GeV) [23] and ^{84}Kr–AgBr (1 A GeV) [present work] reactions from the horizontal SFM analysis. Separate observations of the linear behavior are made in two or three areas for each [23]. For each linear fitting, we assessed the value of χ^2 for each degree of freedom (d.o.f.) and performed linear fitting in the first region to determine the partitioning condition under which the scaling behavior is best shown [23]. Table 1 lists the χ^2 results for each degree of fitting freedom. The optimum linear behavior is indicated by

the minimum values of χ^2 per d.o.f. The best linear fit for the compound particle multiplicity distribution is found at $H = 0.7$, indicating that this is the point at which the anisotropic behavior is most evident [23].

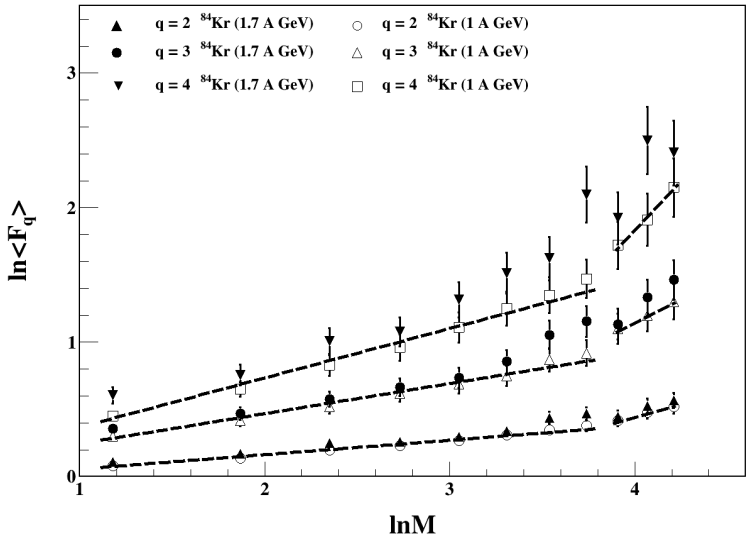

Fig. 1. Correlation of $\ln\langle F_q\rangle$ with $\ln M$ for various orders of the moment at $H = 0.7$ for compound particles emerged from the ^{84}Kr–AgBr (1.7 A GeV) [23] and ^{84}Kr–AgBr (1 A GeV) [present work] reactions for the horizontal analysis.

Table 1. Values of intermittency a_q, χ^2/d.o.f. for fittings at $H = 0.7$ and $H = 1$ compound particles multiplicity distribution for the horizontal analysis.

H	q	a_q	χ^2/d.o.f.	Ref.
0.7	2	0.109 ± 0.008	1.599	[23]
		0.107 ± 0.008	2.028	[Present Work]
	3	0.262 ± 0.019	1.914	[23]
		0.224 ± 0.022	1.682	[Present Work]
	4	0.396 ± 0.034	1.793	[23]
		0.367 ± 0.031	1.712	[Present Work]
1.0	2	0.336 ± 0.007	6.981	[23]
		0.355 ± 0.014	2.963	[Present Work]
	3	0.845 ± 0.017	5.421	[23]
		0.780 ± 0.046	3.375	[Present Work]
	4	1.446 ± 0.030	3.796	[23]
		1.450 ± 0.067	2.249	[Present Work]

In order to compare the self-affine and self-similar behaviors, figure 2 displays the fluctuation of $\ln\langle F_q\rangle$ with $\ln M$ corresponding to $H = 1$ for compound particles emerged from the ^{84}Kr–AgBr (1.7 A GeV) [23] and ^{84}Kr–AgBr (1 A GeV) [present work] reactions from the horizontal SFM analysis. Table 1 also lists the χ^2 value for each linear fitting at $H = 1$ and shows that the scaling behavior is not valid at $H = 1$, as seen by the noticeably high χ^2 values per degree of freedom. At $H = 0.7$, the χ^2 per d.o.f. values of the fits are superior to those at $H = 1$. Thus, the dynamical fluctuation pattern of the multiplicity distribution of compound particles may be described as self-affine rather than self-similar [23].

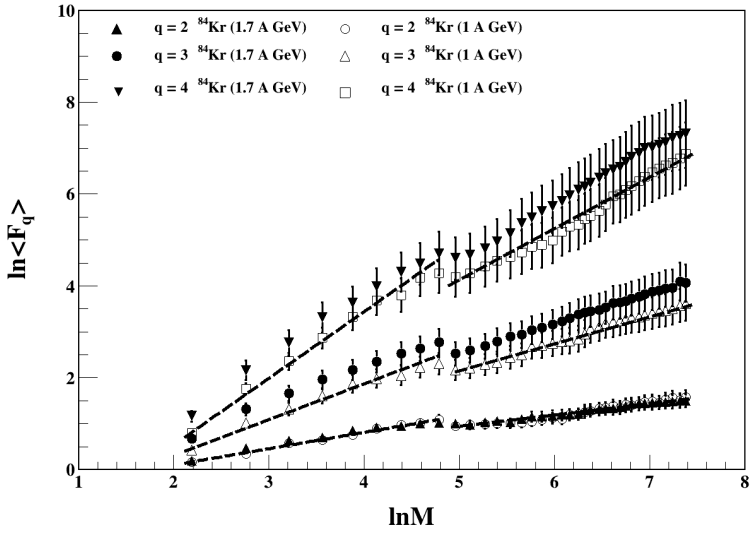

Fig. 2. Correlation of $\ln\langle F_q\rangle$ with $\ln M$ for various orders of the moment at $H = 1.0$ for compound particles emerged from the ^{84}Kr–AgBr (1.7 A GeV) [23] and ^{84}Kr–AgBr (1 A GeV) [present work] reactions for the horizontal analysis.

For the shower particle multiplicity distribution, the entire process is repeated. The horizontal SFM analysis-derived dependents of $\ln\langle F_q\rangle$ on $\ln M$ for various moment orders at $H = 0.6$ and 1 for shower particles emerged from the ^{84}Kr–Em (1.7 A GeV) [23] and ^{84}Kr–Em (1 A GeV) [present work] reactions are displayed in figures 3 and 4, respectively. In Table 2, the corresponding values of χ^2 per d.o.f. are computed and recorded. Table 2 shows that the fluctuation pattern for the shower multiplicity distribution is self-affine rather than self-similar [17, 23].

The linear best fits are made after the $\ln\langle F_q\rangle$ variation and $\ln M$ graphs are created. Exponents of intermittency are retrieved from the linear best fits. Tables 1 and 2 demonstrate that as the order of moment grows, so does

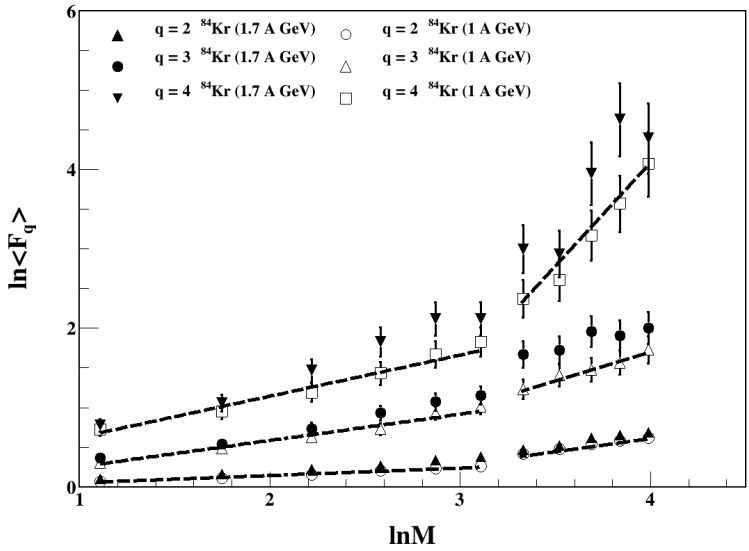

Fig. 3. Correlation of $\ln\langle F_q\rangle$ with $\ln M$ for various orders of the moment at $H = 0.6$ for shower particles emerged from the ^{84}Kr–emulsion (1.7 A GeV) [23] and ^{84}Kr–Em (1 A GeV) [present work] reactions for the horizontal analysis.

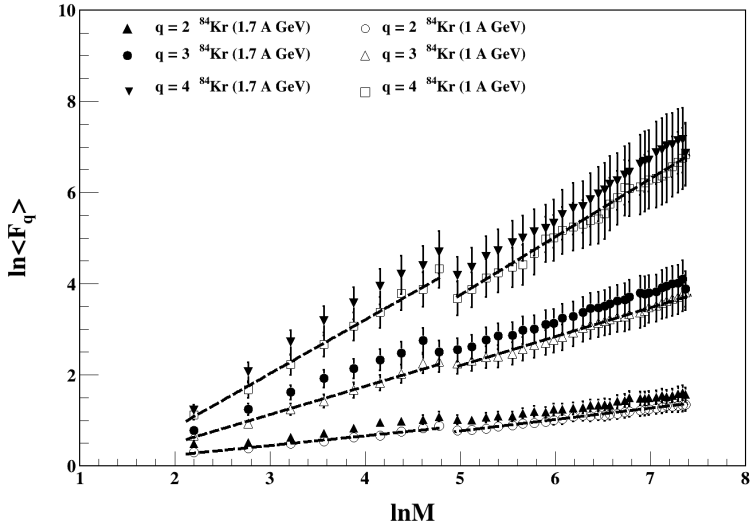

Fig. 4. Correlation of $\ln\langle F_q\rangle$ with $\ln M$ for various orders of the moment at $H = 1.0$ for shower particles emerged from the ^{84}Kr–emulsion (1.7 A GeV) [23] and ^{84}Kr–Em (1 A GeV) [present work] reactions for the horizontal analysis.

Table 2. Values of intermittency a_q, χ^2/d.o.f. for fittings at $H = 0.6$ and $H = 1$ for the shower particle multiplicity distribution for the horizontal analysis.

H	q	a_q	χ^2/d.o.f.	Ref.
0.6	2	0.112 ± 0.007	1.911	[23]
		0.093 ± 0.008	1.567	[Present Work]
	3	0.358 ± 0.022	2.290	[23]
		0.331 ± 0.031	1.565	[Present Work]
	4	0.673 ± 0.044	1.787	[23]
		0.518 ± 0.066	1.633	[Present Work]
1.0	2	0.330 ± 0.004	2.161	[23]
		0.213 ± 0.019	1.736	[Present Work]
	3	0.835 ± 0.011	1.544	[23]
		0.621 ± 0.049	1.294	[Present Work]
	4	1.444 ± 0.022	0.886	[23]
		1.180 ± 0.853	0.864	[Present Work]

the intermittency index [17, 23]. The matching findings of the multiplicity distribution of shower particles and compound particle multiplicity are compared in Tables 1 and 2. We also noticed that the compound particle multiplicity distribution does not have the same H value for the minimal χ^2 per d.o.f. as the shower particle multiplicity distribution.

The fractal pattern [23, 30] in the kinetics of particle creation in their ultimate state is implied by the power-law behavior of the SFMs. Consequently, it makes sense to investigate the fractal character of shower particles generated in the ^{84}Kr–Em collisions and compound particles released from the ^{84}Kr–AgBr reaction under the self-affine scaling scenario [23]. For both fractals and multifractals, the intermittency exponent a_q is connected to the anomalous fractal dimension d_q as [23]

$$d_q = \frac{a_q}{q-1}\,. \tag{9}$$

Figure 5 (a) and (b) illustrates how d_q varies with the order q in the creation of compound particles and shower particles, respectively. As can be seen from the figure, d_q is linearly correlated with order q for shower particles generated in the ^{84}Kr–Em collisions and compound particles released from the ^{84}Kr–AgBr reaction. This implies that the emission of shower particles in the ^{84}Kr–Em collisions and compound particles in the ^{84}Kr–AgBr contacts may be caused by a cascade-type process [23].

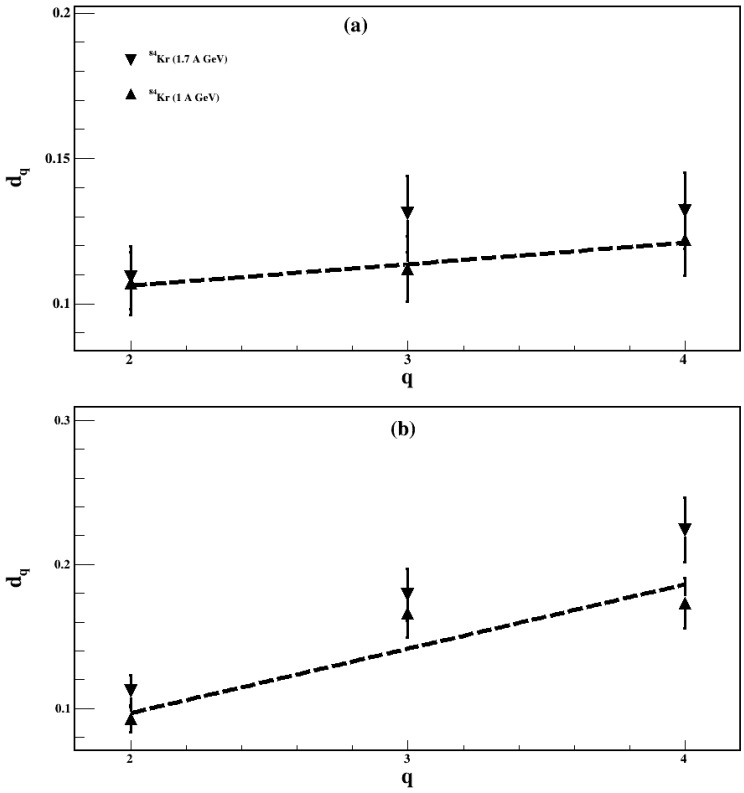

Fig. 5. Correlation of d_q with q for (a) compound particles at $H = 0.7$ emerged from the ^{84}Kr–AgBr (1.7 A GeV) [23] and ^{84}Kr–AgBr (1 A GeV) [present work] reactions and (b) shower particles at $H = 0.7$ emerged from the ^{84}Kr–Em (1.7 A GeV) [23] and ^{84}Kr–Em (1 A GeV) [present work] reactions for the horizontal analysis.

The horizontally-averaged moment depends on the correlation between the cells and is sensitive to the single-particle density distribution's form. Another vertically-averaged factorial moment [31] is normalized locally, meaning it only contains information on fluctuations inside individual cells [23]. For compound particles that formed from the ^{84}Kr–AgBr (1.7 A GeV) [23] and ^{84}Kr–AgBr (1 A GeV) [present work] reactions, respectively, figures 6 and 7 display the fluctuation of $\ln\langle F_2\rangle$ derived from the vertical analysis with respect to $\ln M$ at $H = 0.7$ and $H = 1$. For the ^{84}Kr–AgBr (at 1 A GeV) interactions at $H = 0.7$ and $H = 1.0$, the values of χ^2 per d.o.f. and the intermittency exponents derived from the vertical studies are shown in Table 3. According to the table, the vertical analysis at $H = 0.7$ indicates that the fits' χ^2 per d.o.f. values are better than those at $H = 1$.

Therefore, rather than being self-similar, the dynamical fluctuation pattern of the multiplicity distribution of compound particles may be characterized as self-affine [23].

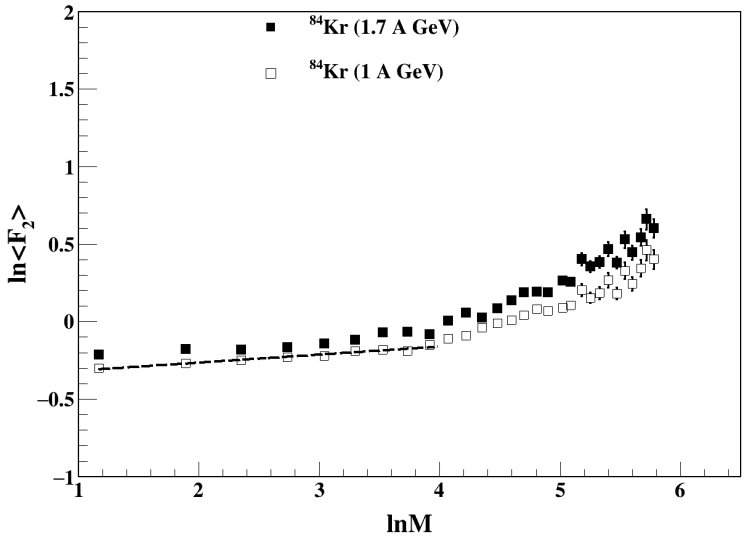

Fig. 6. Correlation of $\ln\langle F_2\rangle$ with $\ln M$ at $H = 0.7$ from the vertical analysis for compound particles emerged from the ^{84}Kr–AgBr (1.7 A GeV) [23] and ^{84}Kr–AgBr (1 A GeV) [present work] reactions.

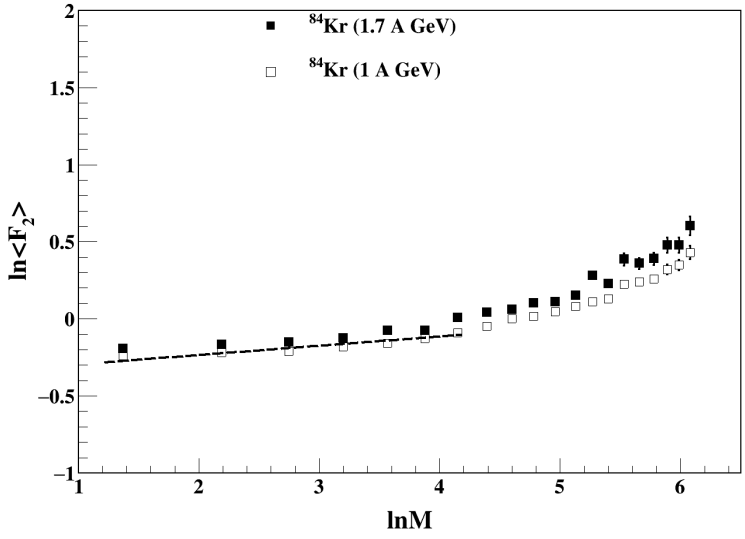

Fig. 7. Correlation of $\ln\langle F_2\rangle$ with $\ln M$ at $H = 1.0$ from the vertical analysis for compound particles emerged from the ^{84}Kr–AgBr (1.7 A GeV) [23] and ^{84}Kr–AgBr (1 A GeV) [present work] reactions.

Table 3. Values of intermittency a_q, χ^2/d.o.f. for fittings at $H = 0.7$ and $H = 1$ compound particles multiplicity distribution for the vertical analysis.

H	q	a_q	χ^2/d.o.f.	Ref.
0.7	2	0.047 ± 0.005	1.390	[23]
		0.052 ± 0.006	1.429	[Present Work]
	3	0.114 ± 0.010	2.072	[23]
		0.125 ± 0.012	2.209	[Present Work]
	4	0.189 ± 0.024	1.570	[23]
		0.208 ± 0.027	1.727	[Present Work]
1.0	2	0.063 ± 0.005	4.036	[23]
		0.060 ± 0.009	3.834	[Present Work]
	3	0.167 ± 0.014	5.302	[23]
		0.159 ± 0.018	5.037	[Present Work]
	4	0.283 ± 0.033	3.832	[23]
		0.269 ± 0.027	3.640	[Present Work]

In the formation of compound particles derived from both vertical and horizontal studies, figure 8 shows how d_q changes with the order q. Figure 8 shows that, for compound particles released from the ^{84}Kr–AgBr (at 1 *A* GeV) interactions, d_q is linearly-dependent on the order q. This implies that the emission of compound particles in ^{84}Kr–AgBr interactions may be caused by a cascade-type process [23].

To reduce background contributions, including fluctuations in total multiplicity, the "mixed event method" is typically applied [32–36]. In this technique, mixed events are formed by randomly picking particles from distinct original events, while keeping the same multiplicity and momentum distributions as the original events. Consequently, rather than employing $F_q(M)$ directly, the following observable is often studied [32]:

$$\Delta F_q(M) = F_q(M)_{\text{data}} - F_q(M)_{\text{mix}}\,, \tag{10}$$

where factorial moments observed in real data are deducted from those derived from mixed events. The $\ln(\Delta F_q)$ reliance on $\ln M$ for different orders of moment for the events that evolved from the ^{84}Kr–Em (1 *A* GeV) [present work] reaction using the mixed event method analysis is shown in figure 9. As previously mentioned, distinct observations of the linear behaviors are made in two or three places for each. For each order of moments, linear fitting is conducted in the first area to find the partitioning condition under which the scaling behavior is best illustrated. In the construction of mixed

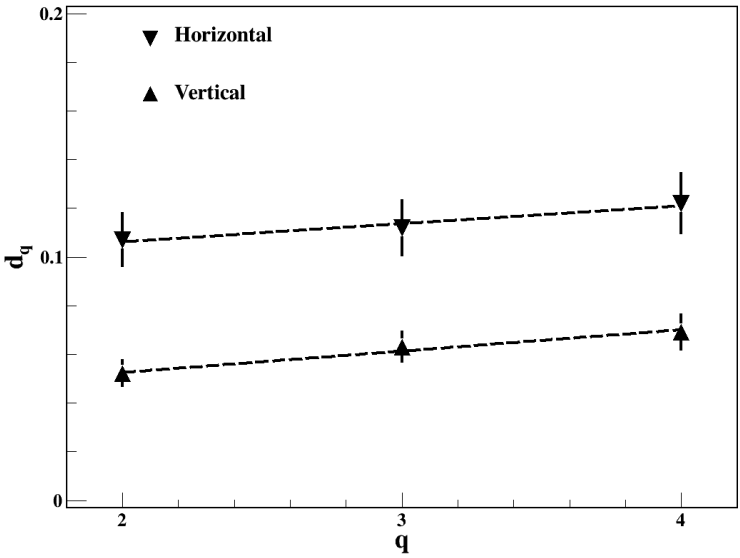

Fig. 8. Correlation of d_q with q for compound particles at $H = 0.7$ emerged from the ^{84}Kr–AgBr (1 A GeV) [present work] reaction.

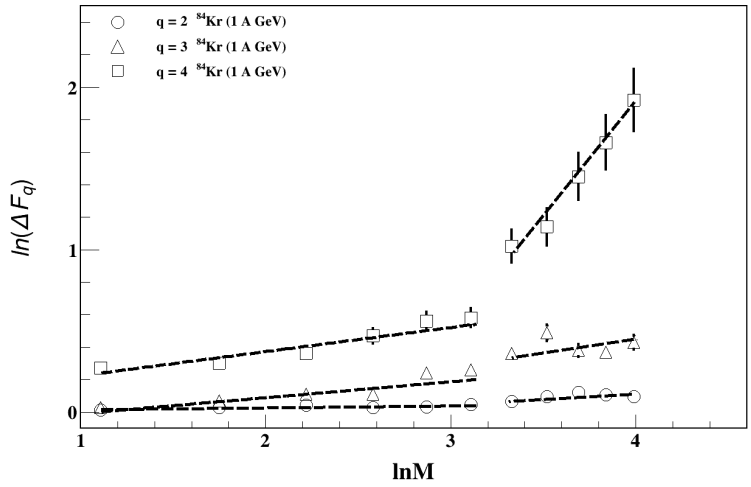

Fig. 9. Correlation of $\ln(\Delta F_q)$ with $\ln M$ for various orders of the moment of the events emerged from the ^{84}Kr–Em (1 A GeV) [present work] reaction analyzed with the mixed event method.

events, true dynamical relationships are mostly eliminated, leaving only statistical fluctuations. Real events contain extra, non-statistical variation that cannot be replicated by mixed events alone, as demonstrated by the fact that $\ln(\Delta F_q)$ is obviously non-zero and grows with $\ln M$. Significant multiparticle

correlation and an intermittent fractal-like pattern in particle generation are suggested by the larger growth of $\ln(\Delta F_q)$ for higher q. Figure 10 demonstrate that d_q fluctuates with the order q in the construction of the mixed event approach. As can be observed from figure 10, d_q is linearly associated with the order q for events created in the ^{84}Kr–Em collisions investigated using the mixed event approach.

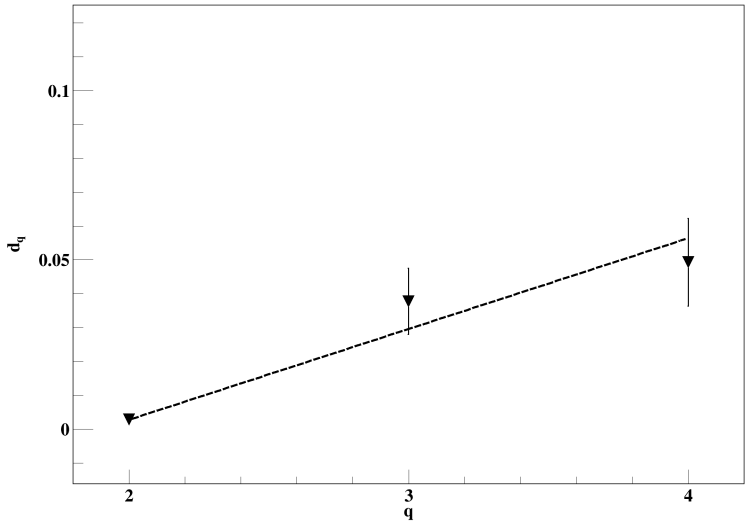

Fig. 10. Correlation of d_q with q for events emerged from the ^{84}Kr–Em (1 A GeV) [present work] reaction analyzed with the mixed event method.

4. Conclusion

It can be inferred from this study that the formation of compound particles from the ^{84}Kr–AgBr reaction and shower particles from the ^{84}Kr–Em reaction at 1 A GeV both exhibit the effects of intermittency. The compound particles utilizing SFM studies reveal the best power-law behavior at $H = 0.7$ in both the vertical and horizontal SFMs analyses, while the shower particle production shows the best power-law behavior at $H = 0.6$ in SFMs analysis. The dynamical variation pattern appears to be self-affine rather than self-similar, according to all of the aforementioned assessments. The unusual fractal dimension of the intermittent behavior has been shown to rise with increasing order of the moment. This implies that multifractality is present in the emission of shower particles from the ^{84}Kr–Em collisions and compound particles from the ^{84}Kr–AgBr reaction.

Authors are thankfull to all the technical staff at the GSI, Germany for exposing the NED plates.

REFERENCES

[1] M.K. Singh *et al.*, «Slow protons emission characteristics with ^{84}Kr + Em interactivity at 1 *A* GeV», *Eur. Phys. J. Plus* **140**, 623 (2025).

[2] B. Kumari, M.K. Singh, R. Singh, «Emission characteristics of the slowest target protons produced in the interaction of ^{84}Kr nuclei with emulsion nuclei at 1 *A* GeV», *J. Korean Phys. Soc.* **84**, 829 (2024).

[3] U. Rawat, M.K. Singh, M. Goyal, «Study the Emission Feature of the Projectile and Target Fragments Using Coulomb Modified Glauber Model and Azimuthal Correlation», *Iran. J. Sci.* **48**, 795 (2024).

[4] J. Boguta, «Baryonic degrees of freedom leading to density isomers», *Phys. Lett. B* **109**, 251 (1982).

[5] H. Weber, M.K. Singh, M. Goyal, «Nucleus–nucleus collisions at high baryon densities», *Phys. Lett. B* **545**, 285 (2002).

[6] H. Stocker, «Collective flow signals the quark–gluon plasma», *Nucl. Phys. A* **750**, 121 (2005).

[7] M.K. Singh *et al.*, «Study of the pseudo-rapidity fluctuations in nucleus–nucleus interactions at relativistic energy», *Indian J. Phys.* **99**, 3429 (2025).

[8] N. Marimuthu, V. Singh, S.S.R. Inbanathan, «Analysis of Various Projectile Interactions with Nuclear Emulsion Detector Nuclei at $\sim$ 1 GeV per Nucleon Using Coulomb Modified Glauber Model», *Adv. High Energy Phys.* **2017**, 7907858 (2017).

[9] M.K. Singh, B. Kumari, «Study of the forward–backward multiplicity correlation at relativistic energy», *J. Korean Phys. Soc.* **86**, 925 (2025).

[10] NA61/SHINE Collaboration (A. Aduszkiewcz *et al.*), «Measurements of total production cross sections for $\pi^+ + \mathrm{C}$, $\pi^+ + \mathrm{Al}$, $K^+ + \mathrm{C}$, and $K^+ + \mathrm{Al}$ at 60 GeV/c and $\pi^+ + \mathrm{C}$ and $\pi^+ + \mathrm{Al}$ at 31 GeV/c», *Phys. Rev. D* **98**, 052001 (2018).

[11] M.K. Singh, B. Kumari, K. Attri, «Utilize azimuthal correlation to examine the collective flow influence caused by the reaction between ^{84}Kr nuclei and emulsion nuclei at 1 *A* GeV», *J. Korean Phys. Soc.* **85**, 560 (2024).

[12] U. Rawat, M.K. Singh, M. Goyal , «Emission characteristics of the shower particles produced in the interaction of ^{84}Kr with emulsion 1 GeV per nucleon», *J. Korean Phys. Soc.* **83**, 411 (2023).

[13] B. Kumari, M.K. Singh, «Forward–Backward Multiplicity Relationship of Target Fragments Produced in the Interaction of $^{84}\mathrm{Kr}_{36}$ + Em at 1 *A* GeV», *J. Phys. Soc. Jpn.* **92**, 124203 (2023).

[14] M.K. Singh, B. Kumari, «Multiplicity correlation of fast target protons and projectile fragments for the events produced in the interaction of ^{84}Kr nuclei with emulsion nuclei at 1 *A* GeV», *Int. J. Mod. Phys. E* **33**, 2450011 (2024).

[15] P.L. Jain, G. Singh, «Factorial, multifractal moments and short-range correlation of shower particles at relativistic energies», *Nucl. Phys.* **596**, 700 (1996).

[16] A.M. Tawfik, «Factorial moments of the multiplicity distribution in Pb+Pb collisions at 158 A GeV», *J. Phys. G: Nucl. Part. Phys.* **27**, 2283 (2001).

[17] D. Ghosh, A. Deb, S. Pal, S. Bhattacharyya, «Evidence of self-affine multiplicity scaling of charged-particle multiplicity distribution in hadron–nucleus interaction», *Pramana J. Phys.* **68**, 789 (2007).

[18] A. Bialas, R. Peschanski, «Moments of rapidity distributions as a measure of short-range fluctuations in high-energy collisions», *Nucl. Phys. B* **273**, 703 (1986).

[19] A. Bialas, R. Peschanski, «Intermittency in multiparticle production at high energy», *Nucl. Phys. B* **308**, 857 (1988).

[20] C.F. Powell, P.H. Fowler, D.H. Perkins, «The Study of Elementary Particles by the Photographic Method», *Pergamon*, Oxford 1959.

[21] B.B. Mandelbrot *et al.*, «Self-Affine Fractal Geometry», in: F. Family, T. Vicsek (Eds.) «Dynamics of Fractal Surfaces», *World Scientific*, Singapore 1991.

[22] A. Bialas, M. Gazdzicki, «A new variable to study intermittency», *Phys. Lett. B* **252**, 483 (1990).

[23] Zhang Dong-Hai, Li Hui-Ling, «Evidence of self-affine multiplicity fluctuation of particle production in Kr–emulsion interactions at 1.7 A GeV», *Chinese Phys. B* **18**, 522 (2009).

[24] L. Liu, Y. Zhang, Y. Wu, «On the random cascading model study of anomalous scaling in multiparticle production with continuously diminishing scale», *Z. Phys. C* **69**, 323 (1995).

[25] L. Liu, Y. Zhan, Y. Deng, «On the influence of momentum conservation upon the scaling behaviour of factorial moments in high energy multiparticle production», *Z. Phys. C* **73**, 535 (1997).

[26] U. Singh, M.K. Singh, V. Singh, «Emission Characteristics of Charged Particle Production in Interactions of ^{84}Kr with the Nuclear Emulsion Detector at Relativistic Energy», *J. Korean Phys. Soc.* **76**, 297 (2020).

[27] Kajal, M.K. Singh, «Emission feature of the singly-charged and doubly-charged projectile fragments emitted in the interaction of $^{84}Kr_{36}$ + Em at 1 GeV per nucleon», *Int. J. Mod. Phys. E* **31**, 2250073 (2022).

[28] S. Kumar, M.K. Singh, V. Singh, R.K. Jain, «Characteristics of the grey particles emission at relativistic energy», *Eur. Phys. J. Plus* **136**, 115 (2021).

[29] W. Ochs, «Multidimensional intermittency analysis», *Z. Phys. C* **50**, 339 (1991).

[30] R.C. Hwa, «Fractal measures in multiparticle production», *Phys. Rev. D* **41**, 1456 (1990).

[31] D. Chanda, M. Kumar Ghosh, A. Mukhopadhyay, G. Singh, «Erraticity analysis of multiparticle production in nucleus–nucleus interactions at relativistic energies», *Phys. Rev. C* **71**, 034904 (2005).

[32] V.Z.R. Ortiz, M. Rybczyński, Z. Włodarczyk, «Scaling for count-in-cell and factorial moment analysis», *Nucl. Phys. B* **1018**, 117051 (2025).

[33] J. Wu *et al.*, «Intermittency of charged particles in the hybrid UrQMD+CMC model at energies available at the BNL Relativistic Heavy Ion Collider», *Phys. Rev. C* **106**, 054905 (2022).

[34] STAR Collaboration (M. Abdulhamad *et al.*), «Energy dependence of intermittency for charged hadrons in Au+Au collisions at RHIC», *Phys. Lett. B* **845**, 138165 (2023).

[35] NA49 Collaboration (T. Anticic *et al.*), «Critical fluctuations of the proton density in A+A collisions at 158 A GeV», *Eur. Phys. J. C* **75**, 587 (2015).

[36] NA49 Collaboration (T. Anticic *et al.*), «Search for the QCD critical point in nuclear collisions at 158 A GeV at the CERN Super Proton Synchrotron (SPS)», *Phys. Rev. C* **81**, 064907 (2010).